Int. J. Electrochem. Sci., 16 **(2021)** Article ID: 210736, doi: 10.20964/2021.07.66

International Journal of
ELECTROCHEMICAL
SCIENCE
www.electrochemsci.org

Short Communication

Poly-ortho-phenylenediamine Modified Pt/Ir Microelectrode as Impedimetric Biosensor

Norazreen Zakaria, Yusairie Mohd, Lim Ying Chin, Muhammad Noor Jalil and Zainiharyati Mohd Zain[*]

Electrochemical Material and Sensor (*EMaS*) Research Group, Faculty of Applied Sciences, Universiti Teknologi MARA, Shah Alam, 40450, Selangor, Malaysia.
[*]E-mail: Zainihar@uitm.edu.my

Received: 1 April 2021 / *Accepted:* 8 May 2021 / *Published:* 31 May 2021

A low impedance between the microelectrode surface and brain biological tissue interface is important for a good signal quality during immunosensor recording to prevent tissue damage during electrical stimulation. The incorporation of a conducting polymer on a microelectrode surface with an internal diameter of 50 µm can significantly reduce the electrode-electrolyte (brain lysate) impedance. An impedimetric immunosensor assay was developed by exploiting the Poly ortho-phenylenediamine (PoPD) conducting properties and has been electrodeposited on the Pt/Ir microelectrode surface. The modified PoPD-Pt/Ir was further biofunctionalised with glutaraldehyde (GA) that act as a crosslinker to mouse monoclonal Aβ antibody (mAβab) immobilisation on PoPD-Pt/Ir. An immunosensor is a simpler and faster method for real-time monitoring of amyloid beta (Aβ40) based on antigen-antibody binding properties compared to the microdialysis technique in a real-time neurochemical study. This Pt/Ir-PoPD-GA- mAβab immunosensor was tested with a trace amount of Aβ40 in the brain tissue lysate sample. Nyquist plots revealed the specific binding of mAβab-amyloid beta (Aβ40) to the biofunctionalised PoPD modified microelectrode surface. Furthermore, proposed equivalent circuits were developed in conjunction with each stage of biofunctionalisation layers on modified Pt/Ir microelectrode to fit and interpret the circuit components that could further explain certain chemical processes and mechanisms of the immunosensor system such as the effect of the electrical component of PoPD film formed during fabrication and its physicochemical properties. The advantages of this needle-like immunosensor include the use of a minimal amount of protein immobilisation reagents with a highly sensitive, selective, and rapid detection technique.

Keywords: Electrochemical Impedance Spectroscopy, Equivalent circuit, Amyloid Beta, Immunosensor, Platinum microelectrode.

1. INTRODUCTION

The impedance characterisation on the microelectrode-electrolyte interface has become important parameters to be observed especially during the construction of implantable biosensors. This

is because low impedance between the surface of the microelectrodes and the electrolyte is required for high-resolution stimulation and recording [1]. High impedance electrodes surfaces would result in a large applied electrode potential leading to undesirable electrochemical reactions that may be harmful to the brain tissue and biological samples [2]. During electrophysiological recording, the brain extracellular signals are low in the form of microvolts for neurons. A high microelectrode surface impedance resulted in the loss of detection of small neural signals due to the noisy signal arises from ion-based electric fluctuations of the surrounding electrolyte media in the brain [3].

Therefore, in order to reduce the impedance on the electrode-electrolyte interface, conducting polymers (CPs) have been widely used for microelectrode surface modification for biosensors and biomedical applications [4-6]. CPs have many advantages because of their ability to self-sealing large amounts of an immobilised enzyme by controlling the thickness of the film [7], efficient charge transfer, homogeneous film-forming during an electropolymerisation, and strong adherence to the electrode surface [8]. In addition, the use of conducting polymer on immunosensor assays may directly immobilise antibodies to the active polymer surface with minimal degradation of antibody functionality. Common CPs that have been previously studied were Poly Pyrrole [9], Poly dopamine-hyaluronic acid [10], Poly thionine [11], Poly ortho-phenylenediamine (PoPD) [12], and others. Among the CPs, PoPD is the promising potential electrode modifier to be applied in the development of brain implantable sensors. In the previous work, PoPD was first electrochemically polymerised on Platinum (Pt) micro discs electrode sites in the form of Pt-PoPD microelectrode [13]. Nevertheless, the capability of Pt/Ir-PoPD microelectrode to permeate PoPD with H_2O_2 and other interferences in the brain has been described previously. The result showed a significant permeability percentage value of Pt/Ir-PoPD towards H_2O_2 compared to other electroactive species in the brain such as ascorbic acid [13].

AC electrochemical impedance spectroscopy (EIS) is a non-destructive method. EIS has been demonstrated to be a method of choice in the discovery of equivalent electrode-electrolyte interface circuit models. Equivalent circuit modelling of EIS data is used to extract physically meaningful properties of the electrochemical system by modelling the impedance data in terms of an electrical circuit composed of ideal resistors (R), capacitors (C), and inductors (L). While other elements such as constant phase element (CPE) and Warburg (Z_w) are often used to specialise the circuit elements, especially in real system applications. This is because these theoretical elements do not necessarily behave in an ideal way with processes that occurred in the actual situation.

Previous researchers have proposed several equivalent circuits to evaluate the electrode-electrolyte interface model coated with polymers [14], metals [15], and organic film [16]. Wu and co-workers used a simple modified Randles equivalent circuit to fit with the impedance measurement for Aβ (1-42) detection on a modified gold thin film. They proposed the elements of R_s (resistance solution), Q_s (CPE between the electrode and nanostructure), R_{nano} (nanostructure resistance), R_{ct} (charge transfer resistance), and Q_{ct} (CPE between protein and nanostructure) [17]. Meanwhile, Szymanska and colleagues have successfully developed a simple equivalent circuit consisting of R_s, bilayer capacitance (C_d), R_{ct}, and Z_w [18]. The equivalent circuit was proposed to study the interaction of the Aβ (1–40) peptide immobilised on the surface of the gold electrode with (−) cotinine and (−) nicotine ditartrate.

Here, PoPD was electropolymerised on the Platinum Iridium (Pt/Ir) disk microelectrode to form a Pt/Ir-PoPD-GA- mAβab immunosensor. In addition, EIS was used to characterise the electrode-

electrolyte interfacial behaviour of the modified microelectrode. The equivalent circuit model that was developed provided the R_s, R_{ct}, Z_w, R_{pore}, and CPE to represent changes from the basis of Pt/Ir bare microelectrode surface to the modification stages of the most outer layers of electrode surface (the antibody, mAβab). The model parameters have been fitted to the experimental results using a nonlinear least-squares fitting.

2. EXPERIMENTAL

2.1. Chemicals and Instrumentations.

Ortho-phenylenediamine (oPD), sodium chloride (NaCl), sodium phosphate monobasic (NaH_2PO_4), Glutaraldehyde (GA), Aβ40 (1.0 mg), and mouse monoclonal antibody (mAβab) (1.5 mg/mL), N-Ethyl-N'-3-Dimethylaminopropyl Carbodiimide (EDC) and N-hydroxysuccinimide (NHS) were purchased from Sigma-Aldrich (Missouri, USA). Sodium hydroxide (NaOH) was supplied by Merck (Darmstadt, Germany). All chemicals were used without further purification. The buffer solution used was phosphate-buffered saline (PBS; pH 7.4, containing 0.1M NaH_2PO_4, 3M NaCl, and 0.9M NaOH). All aqueous solutions were prepared using deionised water (deH_2O) obtained from an Arium® pro purification system (Sartorius, Goettingen, Germany). All electroanalytical measurements were performed using an Autolab PG STAT302 potentiostat/galvanostat (Eco Chemie, Utrecht, The Netherlands) controlled by Nova 1.11 software. A three-electrode electrochemical cell set up consists of a disc-shaped Pt/Ir microelectrode as a working electrode, Pt rod as a counter electrode, and Ag/AgCl as a reference electrode was used in this work.

2.2. Biofunctionalization of the Pt/Ir microelectrode surface.

The surface modification on Pt/Ir microelectrode surface was first carried out by electropolymerisation of PoPD on Pt/Ir bare surface using cyclic voltammetry. The mAβab antibody was then immobilised to Pt/Ir-PoPD using glutaldehyde, EDC, and NHS as described in a previous study [18]. In this study, the immunosensor assay was named Pt/Ir-PoPD-GA- mAβab-Aβ40.

2.3. Aβ40 in brain lysate sample detection.

Sprague-Dawley rat's brain homogenates (adult male; 260−300 g) with experimental treatment groups were obtained from the Collaborative Drug Discovery Research Group, Faculty of Pharmacy, Universiti Teknologi MARA (UiTM), Puncak Alam Campus, Malaysia. Briefly, the Sprague-Dawley rats were injected using a 26-gauge Hamilton syringe into the hippocampus with a standard synthetic Aβ40 in the brain to induce amyloid aggregation in the brain. For this study, the sample of Aβ40 brain tissue lysate solution was prepared with a fixed nominal concentration (5 μg/μL) and was further diluted with 0.3 M PBS solution [19].

2.4. Equivalent circuit modelling.

The models were divided into two types namely process models and equivalent circuit models. These models were fitted from the experimental data to estimate the parameters that adequately describe the fitted data and were further used to analyse the behaviour of the system. In this study, the equivalent circuit models were deliberated based on the three stages of surface biofunctionalisation on Pt/Ir microelectrode, which were i) Pt/Ir microelectrode, ii) Pt/Ir-PoPD, and iii) Pt/Ir-PoPD-GA- mAβab-Aβ40. The comparison between the raw data and the fitting data demonstrates the practical application of this method and was further verified using NOVA 1.11 software indicated by the chi-square (χ^2) fitting test.

3. RESULTS AND DISCUSSION

3.1. Electrochemical characterisation of Pt/Ir and Pt/Ir-PoPD microelectrode.

EIS and cyclic voltammetry (CV) experiments were used in a three-electrode electrochemical cell containing Ag/AgCl as the reference electrode, Pt as the counter electrode, and Pt/Ir, Pt/Ir-PoPD and Pt/Ir-PoPD-GA- mAβab-Aβ40 were the working electrodes immersed in 0.3 M phosphate buffer saline (PBS) at pH 7.4. Fig.1 (a) shows an increased current density on the *I-V* curve of Pt/Ir-PoPD compared to the Pt/Ir bare microelectrode in PBS pH 7.4 suggesting a more conductive PoPD layer formed as stated in a previously published study [19]. Further validation was made using the EIS technique. The Nyquist plots in Fig.1 (b) shows the response of Pt/Ir and Pt/Ir-PoPD microelectrodes in PBS pH 7.4. The polarization potential value was fixed at −0.2 V in the EIS. In addition, -0.2 V was also found to be the optimum potential where the formation of Aβ40–mAβab immune complexes on the microelectrode surface exhibited impedance responses resulting in the appearance of single depressed semicircles in the Nyquist plots [13]. An ideally 90º linear plot (Warburg impedance) at a lower frequency that is controlled by counter-ions diffusion between Pt/Ir bare microelectrode surface in the PBS was observed as shown in Fig.1 (b) [21]. However, the Nyquist plot for Pt/Ir surface that was electrodeposited with PoPD appeared as a double semicircle at a higher and lower frequency. This could be explained by the fact that, at a higher frequency region, the first diameter of the semicircles represented the R_{ct} behaviour between the Pt/Ir microelectrode surface and the PoPD thin film. While the second semicircle appeared at a lower frequency showed that the mass transport towards Pt/Ir-PoPD became limited and the charge accumulation favouring the PoPD film. The obtained Nyquist plot was further evaluated for the calculation of the R_{ct} values extracted from the fitted modified equivalent circuit. The results found that the R_{ct} values obtained with the presence of PoPD on the electrode decreased by 84 % (68.8 ± 3.9 kΩ) compared to the bare electrode (439 ± 0.18 kΩ). The decrease in R_{ct} value can be explained due to the presence of a Pt/Ir bare metal and PoPD polymer interface whereby the initial modification of the bare Pt/Ir microelectrode with PoPD polymer resulted in an enhancement of the surface conductance. This is because PoPD is an excellent conducting polymer. This is further supported by the results obtained from

CV and EIS, which verified that the PoPD enhanced the conductivity of the Pt/Ir microelectrode surface sensing capability.

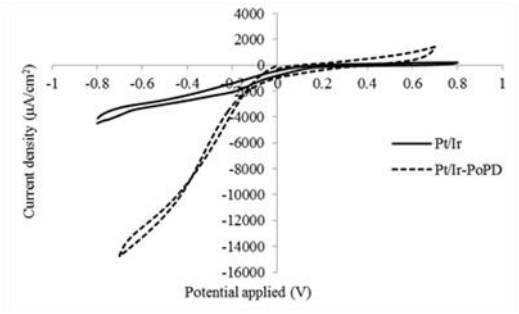

(a)

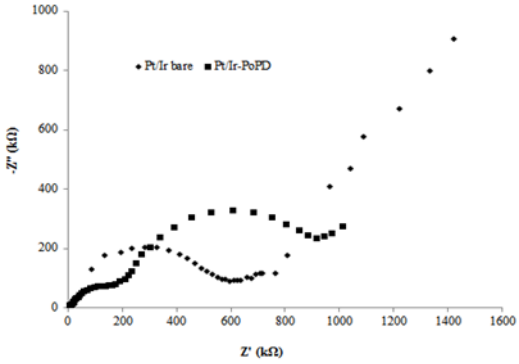

(b)

Figure 1. (a) Cyclic voltammograms of bare Pt/Ir and Pt/Ir-PoPD in 0.3 PBS at 0.01 V/s scan rate, scanning potentials from -0.8 to +0.8 V. (b) Nyquist plots obtained for Pt/Ir microelectrode and Pt/Ir-PoPD performed in 0.3 M PBS at 0.01 V amplitude and frequencies ranging from 0.1 to 10^5 Hz.

3.2. Detection of Aβ40 in the brain lysate.

The bio-recognition mechanism of this biosensor was mainly based on the interaction between the monoclonal antibody (mAβab) and the Aβ40 antigen in the PBS solution. A glutaraldehyde crosslinking was undertaken for the subsequent covalent binding of mAβab to the electrode of Pt/Ir-PoPD surface. An *in vitro* impedimetric was used to detect Aβ40 in the brain lysate. Fig.2 shows the Nyquist plot of Aβ40 detection based on the different electrolyte interactions. The mAβab–GA-PoPD modified Pt/Ir microelectrode or Pt/Ir-PoPD-GA-mAβab immunosensor was immersed in the blank solution (absence of Aβ40), 1 pg/mL standard Aβ40 solution, and 1 pg/mL of Aβ40 spiked in the brain tissue lysate solution. The presence of Aβ40 in electrolyte resulted in a large semi-circle appearance, which is represented by an R_{ct} behaviour compared to a blank solution. An increasing diameter of the semi-circle was observed due to the specific binding of Aβ40 bound on the mAβab–GA-PoPD- modified Pt/Ir microelectrode. This observation revealed that the formation of Aβ40-mAβab immunocomplexes exerted a surface blocking effect and resulted in a reduction of the electron transfer to the Pt/Ir microelectrode. A close loop was observed because the immunosensor involved in the mAβab- Aβ (1-40) bioelectrochemistry is the antibody-antigen specific enzyme-substrate interaction. The specificity

makes the charge transfer mechanism more dominant compared to the diffusion mechanism as seen in our experiment using a 50 µm diameter of Pt/Ir-PoPD microelectrode. Moreover, the existence of this specific binding is confirmed by the affinity binding from the association constant (K_a) values. The Langmuir isotherm approach was utilised to estimate the K_a binding interaction of mAβab towards Aβ40 detection (K_a = 0.915 ± 0.58 pg/mL) with a repetitive number, n=3. The K_a value obtained here was the first indication that the adsorbed Aβ40 to Pt/Ir-PoPD-GA-mAβab electrode is by the specific mAβab–Aβ bio interaction. The R_{ct} value of Aβ40 found in the real brain lysate sample was 161 kΩ, which is slightly lower compared to the 271 kΩ R_{ct} values found in the standard solution. The difference can be attributed to the presence of a small disaggregating solvent in the real samples used in this work that could influence the aggregation process.

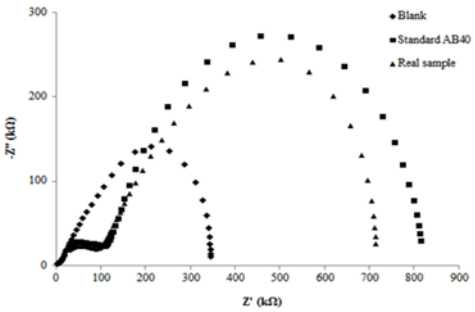

Figure 2. The Nyquist plots of Aβ40 detection in the blank (PBS), 1 pg/mL standard Aβ40, and 1 pg/mL of Aβ40 in the brain tissue lysate on Pt/Ir-PoPD-GA-mAβab immunosensor.

It is worth mentioning that the Aβ40 on Pt/Ir-PoPD-GA-mAβab needle-like microelectrode assay is labelless hence it can be applied as an implantable microelectrode that offers many advantages in the diagnosis and management of Alzheimer's disease compared to neuroimaging technique or psychological analysis [22]. Many reports on the development of amyloid beta biosensors were of larger surface area that is more suitable for *in vitro* studies using screen-printed gold electrode [23] and graphene oxide-gold nanoparticle as the working electrodes [24]. On the other hand, carbon fibre microelectrode of 5 µm tends to bend during the implantation process in the brain [25].

3.3. Equivalent circuit modelling for Pt/Ir bare microelectrode.

Fig. 3 shows the resulting equivalent circuit of Nyquist plot obtained from bare Pt/Ir microelectrode in PBS pH 7.4 buffer indicating the electrode-electrolyte interface behaviour on Pt/Ir bare surface microelectrode. The Nyquist plot starts from a high frequency to a lower limit point frequency. The limiting behaviour at the high and low frequency (ω) could be considered for simplicity in the analysis of the results. Therefore, by plotting the Z_{ima} *vs*. Z_{real}, a circular plot could be produced at $Z_{real}= R_{\Omega} + R_{ct}/2$. Fig.3 shows the equivalent circuit consisting of R_s, R_{ct}, and C_{dl} that is generally fitted to the semi-circle part. However, as the frequency decreased, the linear correlation of Z_{real} and Z_{ima} appeared as a straight line contributing to the semi-infinate diffusion characteristics. The frequency of

this region depends on the Warburg (Z_w) impedance. An equivalent circuit equivalent model for Pt/Ir bare microelectrode in pH 7.4 PBS comprised of Z_w component was added in the previous circuit as the impedance result of Pt/Ir bare microelectrode showed a straight line at a lower frequency region. Nevertheless, the modified equivalent circuit obtained for Pt bare system consisted of a constant phase element (CPE) that was substituted with C_{dl} since Pt/Ir microelectrode exhibited a rougher surface in the real experimental system (SEM micrograph not shown here).

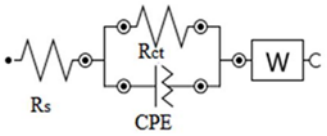

Figure 3. The standard equivalent circuit fitted for Randles-like behaviour obtained from Nyquist plot of Pt/Ir bare microelectrode. (PBS pH 7.4 buffer as electrolyte, Potential = -0.2 V, Frequency: 10 – 10 kHz, Amplitude: 0.01 V).

3.4. Equivalent circuit modelling for Pt/Ir-PoPD in PBS.

After evaluating the electrical properties of the Pt/Ir bare microelectrode, the surface of Pt/Ir microelectrode was electropolymerised with PoPD. As seen in Fig. 4, the Nyquist plot appeared as a double depressed semicircle and an illustration of the modified equivalent circuit was constructed (inset).

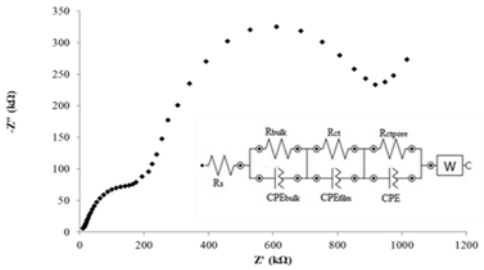

Figure 4. The construction of modified equivalent circuit (inset) on Pt/Ir-PoPD microelectrode. The circuit was developed using NOVA (1.11) software via fit and stimulation analysis.

This circuit model consisted of solution resistance (R_s), film resistance (R_f) from the PoPD film layer on the Pt/Ir microelectrode surface, and pore resistance (R_p). Besides that, the three CPEs present in the modified circuits were CPE_{bulk}, which was contributed by the bulk solution, CPE_{film}, and CPE_{pore}. These elements were presented on the circuit development [26] as follows:

i. Firstly, high impedance corresponds to charge carriers in bulk polymer represented by a parallel combination of R_{bulk} and CPE_{bulk} in series with R_s.

ii. Next, the two parallel combinations of R_{ct} and CPE_{film} in the middle represents the charge transfer between the electrode-polymer interface and polymer-solution interface.

iii. Finally, the last group of element circuit present at a low frequency that is R_{pore} is limited to the pores and roughness on the film. While the effect of the boundary diffusion is displayed by the behaviour represented by the CPE_{pore} element. As the frequency was lowered to 1- 0.1 Hz, the Warburg (Z_w) element was dominant at -45^o and at this stage, the charge transfer of electroactive ions was dependent on the rate at which new electroactive ions diffused with the other electroactive ions that have been oxidised or reduced from the electrode surface to the electrolyte during the measurement time. We hypothesized that the "W" element in Fig. 4 might be due to the H^+ coupled electron transfer reaction with the PoPD molecular layer that covers the microelectrode surface. Here, the W element might not be from the bulk redox species (flavin in mAβab- Aβ (1-40)) bioelectrochemistry because we tested Pt/Ir-PoPD only in PBS. There is an absence of mAβab on the microelectrode surface. The PoPD passivation (layer) on the Pt/Ir microelectrode surface contains phenazine ring ladder-structure with benzenoid and quinoid imine units that react with H^+ from the electrolyte as shown in Equation 1 below [20]:

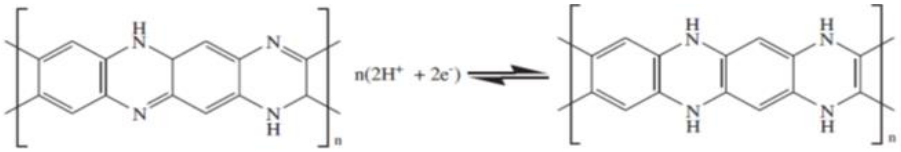

(Eq. 1)

3.5. Modified equivalent circuit for Pt/Ir-PoPD-GA-mAβab-Aβ40

Fig. 5 (a) shows the proposed modified equivalent circuit fitted with the experimental immunosensor electrochemical system consisting of parameters including resistance of the solution (R_s), three elements of CPE which are CPE_{ads}, CPE_{film}, and CPE, Warburg impedance (Z_w), and three elements of R_{ct}. This electrochemical system was deliberated from three circuit components on the modified equivalent circuit where it was due to the protein adsorption resistance (R_{ctads}) at high frequency followed by transport-impeding effects of protein film (R_{ctfilm}) at medium frequency. This is due to the pore resistance (R_{ctpore}) of Pt/Ir microelectrode surface at low frequency. The adsorption of Aβ40 on the microelectrode surface was described as the formation of a current flow barrier with R_{ctads} represented by a partial charge transfer of the strongly adsorbed Aβ40 to the surface and CPE_{ads}. This accounted for the adsorption of electroactive species and charging of the double layer caused by the different active sites on the protein and irregularities on the electrode that produces inhomogeneities at the electrode-electrolyte interface [26]. Since Aβ40 protein was adsorbed on the electrode surface, the electrochemical behaviour was deduced from the parallel combination of $R_{ctads}\|CPE_{ads}$. The reason for this combination was the surface has less free space left on the electrode surface for other electroactive species to be discharged. As a result, a single depressed semicircle appeared after the Aβ40 protein adsorption on the surface of the electrode [26]. A single depressed semicircle of the Nyquist plot as shown in Fig. 5 (b) was observed for protein adsorption. In order to model an equivalent circuit correlated with protein adsorption, the adsorption-limited interfacial kinetics of electroactive proteins were considered during the circuit development [27].

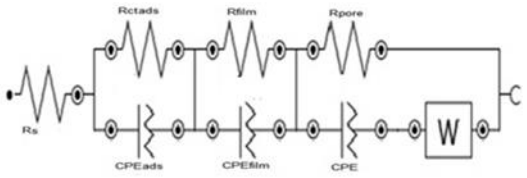

(a)

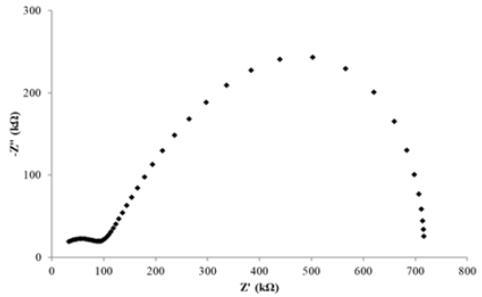

(b)

Figure 5. The construction of modified equivalent circuit from Nyquist plot obtained on Pt/Ir-PoPD-GA- mAβab- Aβ40 immunosensor. The circuit (a) was developed using NOVA (1.11) software via fit and stimulation analysis.

All equivalent circuits resulted in low chi-square $\chi 2$ values (less than 0.01) representing a good fitting of experimental Nyquist plots towards the modelled equivalent circuits.

4. CONCLUSION

The biofunctionalisation with GA, EDC, and NHS following the electropolymerisation of PoPD on the Pt/Ir microelectrode surface has been characterised by EIS and CV techniques. The equivalent circuits proposed here revealed that there has been a conductance enhancement supported by the AC impedance spectrum. It is important to understand the electrochemical system to portray an equivalent circuit so that the circuit can be properly fitted and measured. Hence, this Pt/Ir microelectrode and the characteristics of the PoPD films could suggest the potential use of this kind of implantable needle-like microelectrode in other neurochemical biosensor developments.

ACKNOWLEDGEMENT
This research was financially supported by the Ministry of Education, Malaysia in the form of an FRGS grant (600-IRMI/FRGS 5/3 (106/2019).

References

1. A. Abdurrahman, D. Price and S. Bhansali, *Sens. Actuators B: Chem*, 127 (2007) 89.
2. N. Kotov, J. Winter, I. Clements, E. Jan, B. Timko, S. Campidelli, S.Pathak, A. Mazzatenta, C. Lieber, M. Prato, R. Bellamkonda, G. Silva, N. Kam, F. Patolsky and L. Ballerini, *Adv. Mater.*, 21, 40 (2009) 3970.

3. W. Franks, I. Schenker, P.Schmutz and Hierlemann, *IEEE, Trans. Biomed*, 52 (2005) 1295.
4. R. Garjonyte and Malinauskas, *Sens. Actuators B*, Chem., 63 (2000) 126.
5. C. Andrew, B. G.Z. Garifallou., F. Davis, D.Stuart, Collyer ,G. Tsekenis, P. A. Millner, T.D. Gibson and P. J. Sé amus Higson, *Biosens.Bioelectron.*,24, 5 (2009) 1090.
6. G. Scandurra, A. Arena, C. Ciofi and G.Saitta, *Sensors*, 13, 3 (2013) 3878.
7. C. Wu and H. Chang, *Anal. Chim. Acta*, 505, 2 (2004) 269.
8. F. Terzi, L. Pasquali and R. Seeber, *Anal. Bioanal. Chem.*, 405, 5 (2013) 1513.
9. I. D. L. F. Salas, Y. Sudhaka and M. Selvakumar, *Appl. Surf. Sci.*, 296 (2014) 195.
10. L. Zhang, H. Yin, J. Luo, P. Yang, and J. Cai, *Chinese J. Anal. Chem.*, 41, 4 (2013) 534.
11. M. Rahman, X. Li ,J. Kim, B. Lim, A. Ahammad and J. Lee, *Sens.Actuators* B, Chem., 202, (2014) 536.
12. J. Han, H. Boo, S. Park and T. Chung, *Electrochim. Acta*, 52, 4, (2006) 1788.
13. Z M. Zain and N. Zakaria, *Malaysian J. Anal. Sci.*, 18, 1 (2014) 107.
14. A. Reza and C. David, *Biomaterials*, 29, 9 (2008) 1273.
15. R. Hrdy, H. Kynclova, J. Drbohlavova, V. Svatos and J. Chomoucka, *Int. J. Electrochem. Sci*., 8 (2013) 4384.
16. J. Yu and C.C Liu, *Sensors*, 10 (2010) 5345.
17. C. Wu, B. Ku,C. Ko, C. Chiu, G. Wang, Y. Yang and S. Wu, *Electrochimica Acta,* 134 (2014) 249.
18. I. Szymańska, H. Radecka, J. Radecki and R. Kaliszan, *Biosens. Bioelectron.* 26, 9 (2007) 1955.
19. N. Zakaria, M. Ramli, K. Ramasamy, K.L. Meng, C. Yean, B. Singh, Z.M. Zain and K.F. Low, *Anal. Biochem.*, 555 (2018)12.
20. P.Muthirulan, N. Kannan and M. Meenakshisundaram, *J. Adv. Res.*, 4 (2013) 385.
21. X.M. Miao, R. Yuan, Y.Q. Chai, Y.T. Shi and Y.Y. Yuan, *J. Electroanal. Chem.*, 612, 2 (2008) 157.
22. V. Serafin, M. Gamella, M. Pedrero, A. Montero-Calle, C.A. Razzino, P. Yanez-Sadeno, R. Barderas, S. Campunzo and J.M. Pingarron, J. Pharm. and Biomed. Analysis 189 (2020) 113437.
23. J. V. Rushworth, A. Ahmed, H.H. Griffiths, N.M. Pollock, N.M. Hooper and P. A. Miller, *Biosens Bioelectron*., 56 (2014) 83.
24. I. Sun, Y. Zhong, J. Gui, X. Wang, X. Zhuang, J. Weng, *J. Nanomedicine*, 13 (2018) 843.
25. S. Prabhulkar, R. Piatyszek, J.R. Cirrito, Z.Z. Wu and C.Z. Li, *J. Neurochem*., 122 (2012) 374.
26. V.F. Lvovich, Impedance Spectroscopy: Application to Electrochemical and Dielectric Phenomena, Wiley, New Jersey, 2012.
27. E. Katz and I. Willner, *Electroanalysis*, 15(2003) 913.